

# Specific Heat Exponent for the 3-d Ising Model from a 24-th Order High Temperature Series.

*by*

Gyan Bhanot<sup>1,2</sup>, Michael Creutz<sup>3</sup>,  
Uwe Glässner<sup>4</sup>, Klaus Schilling<sup>4</sup>

## ABSTRACT

We compute high temperature expansions of the 3-d Ising model using a recursive transfer-matrix algorithm and extend the expansion of the free energy to 24th order. Using ID-Padé and ratio methods, we extract the critical exponent of the specific heat to be  $\alpha = 0.104(4)$ .

---

<sup>1</sup>Thinking Machines Corporation, 245 First Street, Cambridge, MA 02142, USA

<sup>2</sup>Institute for Advanced Study, Princeton, NJ 08540, USA

<sup>3</sup>Brookhaven National Laboratory, Upton, NY 11973, USA

<sup>4</sup>Physics Department, University of Wuppertal, Gausstrasse 20, 42097 Wuppertal, Germany

# 1 INTRODUCTION

High- and low-temperature expansions constitute major tools for the calculation of critical properties in statistical systems. The Ising and Potts model low temperature expansions were recently extended [1, 2, 3, 4] using a technique based on the method of recursive counting [5]. In a separate development, Vohwinkel [6] implemented the shadow-lattice technique of Domb [7] in a very clever way and added many new terms to the series. However, the extraction of critical parameters from low temperature series is hampered by the presence of unphysical singularities. This is especially true of the 3-d Ising model. For this reason, low temperature analytic methods are very often inferior to Monte-Carlo methods for computing critical exponents.

High-temperature (HT) expansions on the other hand, generally have better analytic behavior and yield more accurate exponents. Very recently, two variants of the recursive counting technique for HT expansions have been pursued. While Enting and Guttmann [4] keep track of spin configurations on a set of rectangular finite lattices, ref.[3] counts HT-graphs on finite, helical lattices. Such computer based series expansions have very large memory requirements. This makes them ideal candidates for large parallel computers if communication issues can be handled efficiently. In this paper we will present the results of a HT expansion of the 3-d Ising model to 24th order, obtained on a 32 node 1 GByte Connection Machine CM-5. The implementation is based on a bookkeeping algorithm of binary coded spin configurations in helical geometry.

# 2 COMPUTATION OF THE SERIES

We start with a discussion of the HT algorithm to compute the partition functions on finite 3-d Ising lattices. Starting from the action

$$E\{s\} = - \sum_{\langle i,j \rangle} s_i s_j , \quad (1)$$

the partition function is

$$Z = \sum_{\{s\}} \exp(-\beta E) = \sum_{\{s\}} \prod_{\langle i,j \rangle} \exp(\beta s_i s_j) \quad (2)$$

and is expanded in a HT series [8]

$$Z = (\cosh^3 \beta)^V \sum_{\{s\}} \prod_{\langle i,j \rangle} (1 + s_i s_j t) = (2 \cosh^3 \beta)^V \sum_k p(k) t^k , \quad (3)$$

with the HT expansion parameter  $t = \tanh \beta$ .  $V$  is the volume of the system. The free energy per spin is defined as

$$f = -\frac{1}{\beta V} \log Z = -\frac{2 \cosh^3 \beta}{\beta} - \frac{1}{\beta} \sum_k f_k t^k . \quad (4)$$

For simplicity, consider a finite simple cubic lattice which, in the recursion algorithm, is built up by adding one site after the other, layer by layer. This procedure defines the

recursion step, which requires knowledge only of those spin states that are contained in the exposed two-dimensional surface layer. To minimize finite size effects, it is best to use helical boundary conditions [2, 3]. One can visualize helical boundary conditions by imagining all spins in the layer laid out along a straight line. In this picture, the nearest neighbours to a given site in the sequence in the  $i$ th direction can be chosen to be  $h_i$  sites away, with  $i = x, y, z$ . It is convenient to assume  $h_x < h_y < h_z$ . It is easy to see that as spins are added, one needs only to keep track of the states of spins on the topmost  $h_z$  sites. Let these spins be denoted  $s_1, \dots, s_{h_z}$ . Then the partition function can be rewritten as

$$Z = (2 \cosh^3 \beta)^V \sum_k \sum_{s_1, \dots, s_{h_z}} p(k; s_1, \dots, s_{h_z}) t^k . \quad (5)$$

The recursion step, which consists of adding another spin  $s_0$  to the system, changes the partition function into

$$\begin{aligned} Z &= 2^V (\cosh^3 \beta)^{V+1} \sum_{s_0} \sum_k \sum_{s_1, \dots, s_{h_z}} p(k; s_1, \dots, s_{h_z}) t^k \\ &\times (1 + s_0 s_{h_x} t) (1 + s_0 s_{h_y} t) (1 + s_0 s_{h_z} t) . \end{aligned} \quad (6)$$

$s_{h_x}, s_{h_y}$  and  $s_{h_z}$  are the backward nearest neighbours of the site  $s_0$ . The site  $s_0$  will displace its backward  $z$  neighbour site  $s_{h_z}$  after the counting of the added spin is completed. Since  $s_{h_z}$  will not be referred to in the subsequent steps of the algorithm, the summation over  $s_{h_z}$  can be carried out:

$$\begin{aligned} Z &= 2^V (\cosh^3 \beta)^{V+1} \sum_{s_0} \sum_k \sum_{s_1, \dots, s_{h_z-1}} \\ &\times [ +p(k; s_1, \dots, s_{h_z-1}, s_0) t^k (1 + s_0 s_{h_x} t) (1 + s_0 s_{h_y} t) (1 + t) \\ &\quad + p(k; s_1, \dots, s_{h_z-1}, \bar{s}_0) t^k (1 + s_0 s_{h_x} t) (1 + s_0 s_{h_y} t) (1 - t) ] . \end{aligned} \quad (7)$$

The contribution in the second (third) line of this equation contains the part with  $s_{h_z}$  being parallel (antiparallel, denoted by  $\bar{s}_0$ ) to  $s_0$ . Comparing this expression with the HT series (5) for the new system yields the recursion relation induced for the coefficients  $p$ :

$$\begin{aligned} 2p'(k; s_0, s_1, \dots, s_{h_z-1}) &= p(k-0; s_1, \dots, s_{h_z-1}, s_0) \\ &+ p(k-0; s_1, \dots, s_{h_z-1}, \bar{s}_0) \\ &+ p(k-1; s_1, \dots, s_{h_z-1}, s_0) (s_0 s_{h_x} + s_0 s_{h_y} + 1) \\ &+ p(k-1; s_1, \dots, s_{h_z-1}, \bar{s}_0) (s_0 s_{h_x} + s_0 s_{h_y} - 1) \\ &+ p(k-2; s_1, \dots, s_{h_z-1}, s_0) (s_{h_x} s_{h_y} + s_0 s_{h_x} + s_0 s_{h_y}) \\ &+ p(k-2; s_1, \dots, s_{h_z-1}, \bar{s}_0) (s_{h_x} s_{h_y} - s_0 s_{h_x} - s_0 s_{h_y}) \\ &+ p(k-3; s_1, \dots, s_{h_z-1}, s_0) (s_{h_x} s_{h_y}) \\ &+ p(k-3; s_1, \dots, s_{h_z-1}, \bar{s}_0) (-s_{h_x} s_{h_y}) \end{aligned} \quad (8)$$

It is crucial to remove finite-size errors by combining the results of different lattice structures as described in refs. [2, 3]. We use the set of lattices listed in table 1 and obtain the free energy coefficients up to 24th order as given in table 2. In order to eliminate the contribution from (unphysical) loops with an odd number of links in any direction, we use

$h_x$	9	1	9	5	7	10	5	14	11	14	9	9	5	5	16	10	16	1	17
$h_y$	11	12	14	15	15	13	15	15	16	16	17	16	17	19	17	19	20	18	21
$h_z$	13	14	16	16	16	17	17	17	17	17	19	20	20	20	21	21	21	22	22
$w$	-3	3	-3	-3	3	-3	3	-3	3	3	-1	-2	-1	1	-2	5	2	-2	2

Table 1: Structures and weights  $w$  of the lattices used

order $k$	free energy $f_n$
0	0
2	0
4	3
6	22
8	$375/2$
10	1980
12	24044
14	319170
16	$18059031/4$
18	$201010408/3$
20	$5162283633/5$
22	16397040750
24	266958797382

Table 2: Free energy up to 24th order

the cancellation technique of ref. [3]. This amounts to inserting additional signature factors into eq. 6 for each of the three link-factors

$$(1 + s_0 s_{h_i} t) \rightarrow \sigma_i (1 + s_0 s_{h_i} t) , \quad i = x, y, z \quad (9)$$

with  $\{\sigma_x, \sigma_y, \sigma_z\} = \{\pm, \pm, \pm\}$ . By performing 8 separate runs corresponding to all possible values of  $\vec{\sigma}$  and adding the results, one achieves a complete elimination of the unwanted loops. Possible contributions of higher-order finite-size-loops are at least of order 25 for this set of lattices. Since we use open boundary conditions, the coefficients  $p$  are invariant under the global transformation  $s_i \rightarrow -s_i$ . This  $Z(2)$  symmetry enables us to reduce memory requirements by a factor of two. Unlike refs. [2, 3, 4] we use multiple-word arithmetic to account for the size of the coefficients. This implementation needs about 100% more memory but leads to a doubling in performance. Since the number of words can be adjusted separately for every order, the computational effort can be reduced accordingly. On the 32 node CM-5 the total time for all computations was about 50 hours.

Compared to the finite-lattice approach of Enting and Guttmann [4], our method appears to require more CPU-time since we need to cancel unphysical loops. It should be noted, however, that helical lattices are very naturally implemented in data parallel software environments and thus lead to better performance. In the usual finite lattice method [4], the HT expansion can only be extended in fairly coarse steps, using lattices with  $(4 \times 5)$  cross-section for 22nd order and  $(5 \times 5)$  cross-section for 26th order, respectively. For this reason, a 24th order computation would not have been feasible using that method with our computer resources.

### 3 CRITICAL EXPONENT

The specific heat is defined as

$$c|_{h=0} = \beta^2 \frac{\partial^2}{\partial \beta^2} \log Z = \sum_k c_k t^{2k} \quad (10)$$

and is expected to behave near  $T_C$  as

$$c|_{h=0} = A(T) |T - T_C|^{-\alpha} \left[ 1 + B(T) |T - T_C|^\theta + \dots \right] , \quad (11)$$

with  $A$  and  $B$  being analytic near  $T_C$  [9, 10]. We analyse the series using unbiased and biased inhomogeneous differential Padé-approximants (IDPs) [11] as well as ratio-tests.

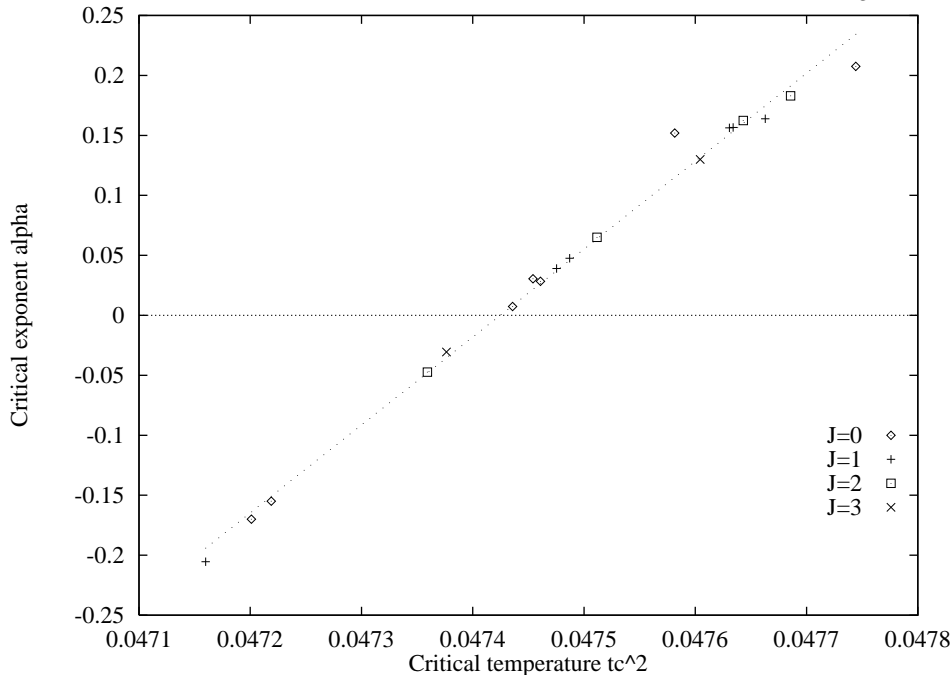
#### 3.1 Padé-Analysis

In figure 1 we plot  $\alpha$  against  $t_C^2$  for each IDP-Approximant [J/L;M]. Fitting the linear dependence of  $\alpha$  on  $t_C^2$  [9], we find

$$\alpha = 0.102 \pm 0.008 \quad (12)$$

at the value  $t_C = 0.218092$  as obtained in Monte-Carlo simulations [12]. A direct, biased-IDP analysis was also performed. We obtained  $\alpha = 0.109 \pm 0.016$ .

Figure 1: Critical exponent  $\alpha$  as a function of  $t_C^2$ .



IDPs can also be used to predict the most significant digits of the next term in the specific heat series [4]. The estimate of the 24th order term as obtained in ref. [4] agrees perfectly with our exact result. Using the same method we can estimate the 26th order term in the expansion to be

$$f_{26} = 443762(4) \times 10^7, \quad (13)$$

where the errors quoted are two standard deviations.

### 3.2 Ratio-Test

The main problem in the determination of critical exponents in the low-temperature case is the presence of unphysical singularities nearer to the origin than the physical one. Since the expansion coefficients  $c_n$  are dominated by these unphysical singularities, ratio-methods cannot be applied.

In the HT-expansion, the physical singularity dominates the asymptotic behaviour, so that the ratio  $r_n = c_n/c_{n-1}$  of successive coefficients of the series is expected to behave as [9]

$$r_n = \frac{1}{t_C^2} \left( 1 + \frac{\alpha - 1}{n} + \frac{c}{n^{1+\theta}} + \frac{d}{n^{1+2\theta}} + O\left(\frac{1}{n^{1+3\theta}}\right) \right). \quad (14)$$

Assuming that the correction-to-scaling exponent  $\theta$  is close to 0.5 [12, 13], the following sequence  $s_n$  is expected to converge towards  $\alpha$  like

$$s_n := \left( t_C^2 r_n - 1 \right) n + 1 = \alpha + \frac{c}{n^{1/2}} + \frac{d}{n} + O\left(\frac{1}{n^{3/2}}\right). \quad (15)$$

A plot of this sequence against  $n$  is shown in figure 2. Obviously the first four values are

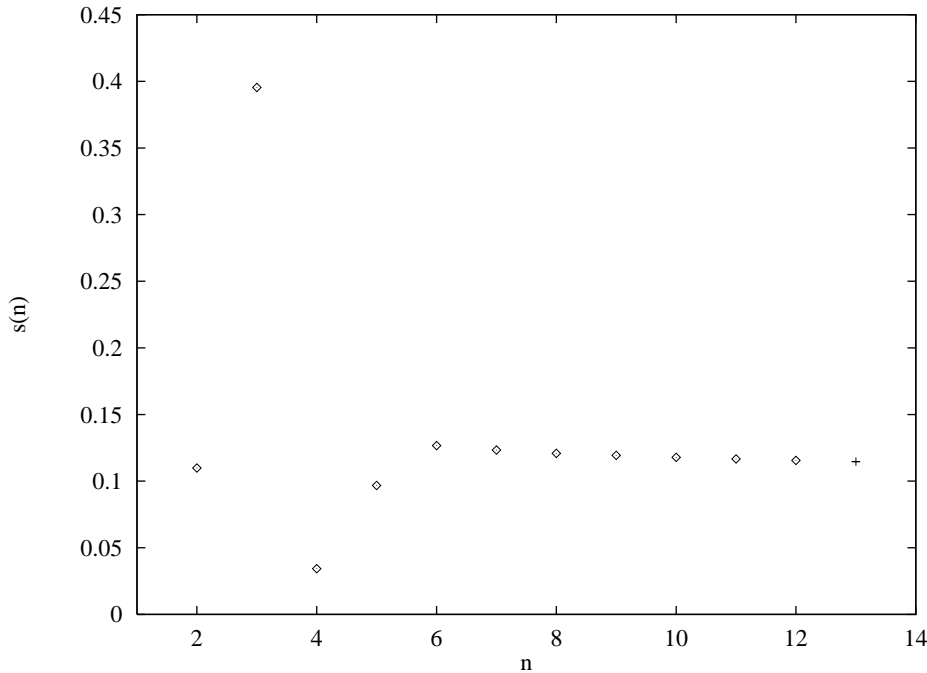


Figure 2: Plot of the sequence  $s_n$  against  $n$ . The error of  $s_{13}$ , obtained from the ID-Padé extrapolation, is too small to be visible.

dominated by higher order corrections. To obtain estimates for  $\alpha$  we therefore use only the values  $\{s_6, \dots, s_{13}\}$ . A 3-parameter least-square-fit using the ansatz of eq. (15) yields the values shown as diamonds in figure 3. The value of  $\alpha = 0.113$  obtained by the fit to the points  $\{s_6, \dots, s_{11}\}$  is in perfect agreement with the result of ref. [4]. Their estimate of  $\alpha = 0.110$  using the extrapolated term  $s_{12}$  appears to be slightly above our value of  $\alpha = 0.108$  using the exact term. Including our value for  $s_{13}$  of the ID-Padé extrapolation eq. (13) we obtain  $\alpha = 0.105(2)$ . The error represents the uncertainty of the extrapolation. However, from fig. 3 it is quite suggestive that the  $\alpha$ -values might converge to a value below 0.105.

To get an estimate of the uncertainties of our results, we investigate the stability of the fits. For this purpose, we repeat the analysis after eliminating the point  $s_6$  from the data. As a result we obtain sizeable changes for  $\alpha$ . The new data are shown as crosses in fig. 3.

In figure 4 we present the results for the first correction-to-scaling coefficient  $c$  from our 3-parameter fits. In contrast to ref. [4], our values suggest that  $c$  changes sign with increasing  $n_{max}$ . Because of the sensitivity of the fits to the number of terms we keep, it is difficult to determine the value of  $c$  very precisely. Our best estimate is  $c = 0.01(4)$ . Since  $c$  vanishes within error, it seems reasonable to also try a 2-parameter-ansatz with  $c = 0$  to fit the data. The results of these fits are shown in figure 5. We now find that the fits are much more stable and the  $\alpha$  estimates show much more of a convergence to their asymptotic values. The best value (from the largest  $n_{max}$ ) is  $\alpha = 0.1045(3)$ . This value supports the impression of the 3-parameter fits, which suggested that  $\alpha$  was slightly below 0.105. Taking into account the fact that neglecting  $c$  causes a systematic error, our final

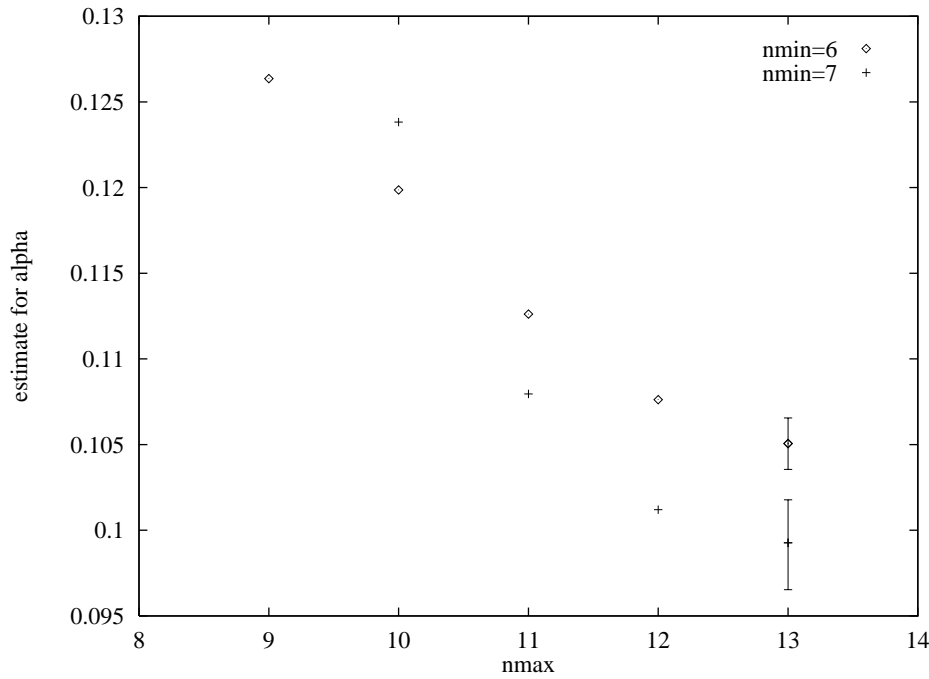


Figure 3: Estimates of alpha using a 3-parameter-fit. Each point represents the results of a fit to the set of values  $\{s_{n_{min}}, \dots, s_{n_{max}}\}$ . The error bars of the rightmost values represent the uncertainty of the extrapolated 13th term.

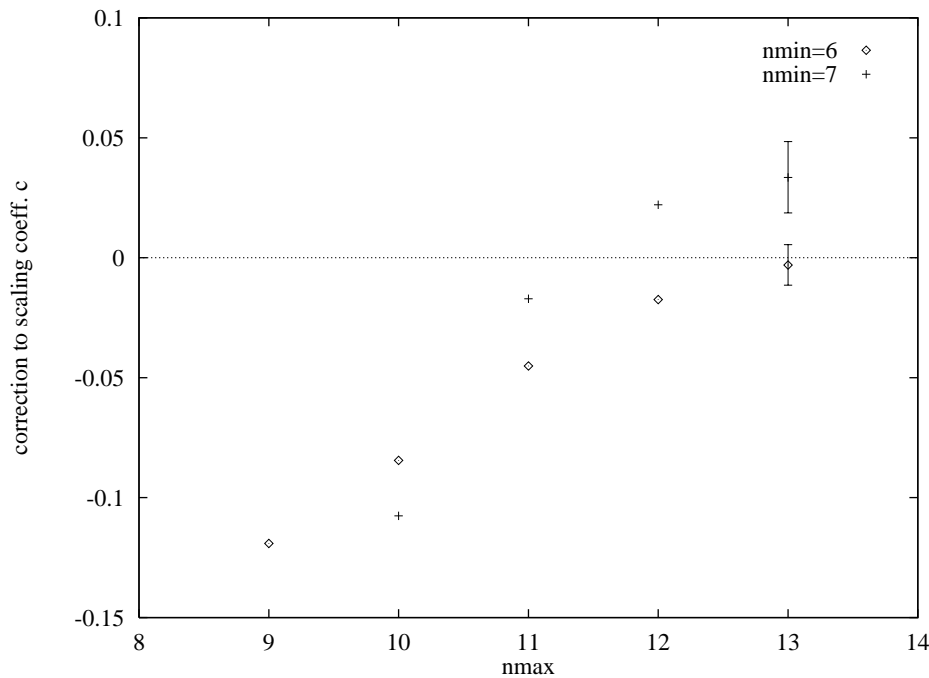


Figure 4: Estimates of c using a 3-parameter-fit. Each point represents the results of a fit to the set of values  $\{s_{n_{min}}, \dots, s_{n_{max}}\}$ . The error bars of the rightmost values represent the uncertainty of the extrapolated 13th term.

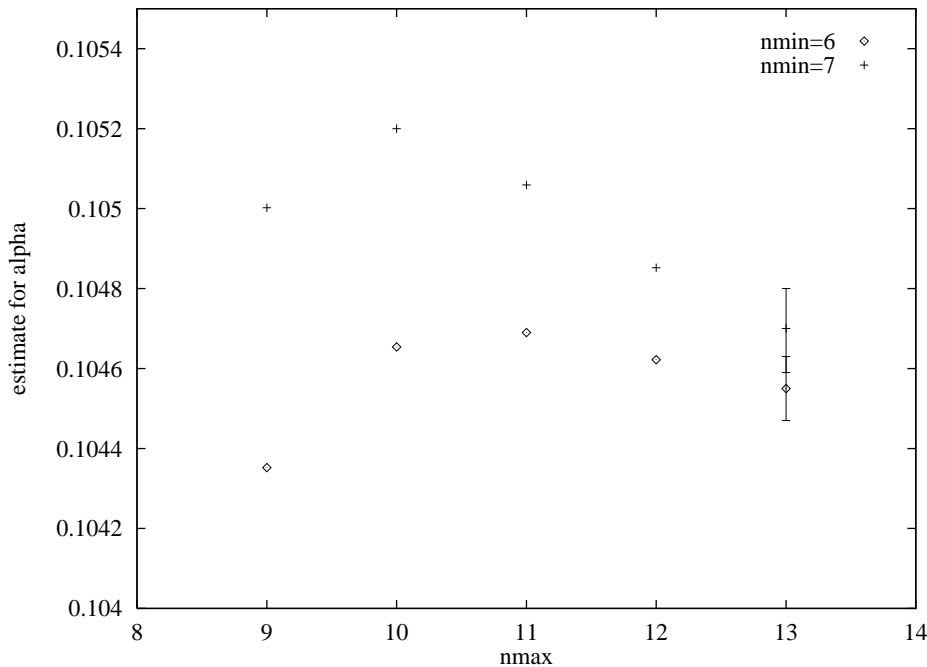


Figure 5: Estimates of  $\alpha$  using a 2-parameter-fit with  $c = 0$ . Each point represents the results of a fit to the set of values  $\{s_{n_{min}}, \dots, s_{n_{max}}\}$ . The error bars of the rightmost values represent the uncertainty of the extrapolated 13th term.

estimate for the critical exponent is,

$$\alpha = 0.104(4) . \quad (16)$$

## 4 DISCUSSION AND OUTLOOK

The crucial element in the estimate of the error in  $\alpha$  ( eq. 16 ) is our neglect of the correction-to-scaling coefficient  $c$ . The resulting systematic error is rather large. From fig. 4 one might speculate that the estimates for  $c$  begin to exhibit asymptotic behaviour at the 26th order. Therefore an exact calculation of the 26-th term of the expansion might reduce the uncertainty of  $c$  significantly. If the magnitude of  $c$  turns out to be really negligible, one could adopt the errors of the linear fits, and  $\alpha$  would be obtained accurate to the fourth significant digit.

## 5 ACKNOWLEDGEMENTS

This work was partly funded under Contracts No. DE-AC02-76CH00016 and DE-FG02-90ER40542 of the U.S. Department of Energy. Accordingly, the U.S. Government retains a nonexclusive, royalty-free license to publish or reproduce the published form of this contribution, or allow others to do so, for U.S. Government purposes. The work of GB was also partly supported by a grant from the Ambrose Monell Foundation. UG and KS are grateful to Deutsche Forschungsgemeinschaft for its support to the Wuppertal CM-Project.

## References

- [1] M. Creutz, Phys. Rev. **B43** (1991) 10659.
- [2] G. Bhanot, M. Creutz and J. Lacki, Phys. Rev. Letters **69** (1992) 1841; G. Bhanot, M. Creutz, I. Horvath, U. Glässner, J. Lacki, K. Schilling, J. Weckel, Phys. Rev. **B48** (1993) 6183.
- [3] G. Bhanot, M. Creutz, I. Horvath, J. Lacki and J. Weckel, Preprint IASSNS-HEP-93/11, to appear in Phys. Rev. E.
- [4] A.J. Guttmann and I.G. Enting, J.Phys. **A26** (1993) 807.
- [5] K. Binder, Physica **62** (1972) 508; G. Bhanot, J. Stat. Phys. **60** (1990) 55; G. Bhanot and S. Sastry, J. of Stat. Phys. **90** (1990) 333.
- [6] C. Vohwinkel, Phys. Lett. **B301** (1993) 208.
- [7] C. Domb, **Ising Model**. In: C. Domb and M.S. Green (eds) Phase Transitions and Critical Phenomena, Vol. **3** (Academic Press, New York).
- [8] G. Parisi, **Statistical Field Theory**, Frontiers in Physics Series, No. 66, (Addison-Wesley, Reading, Mass.).
- [9] A.J. Guttmann, **Asymptotic Analysis of Power Series Expansions**. In: C. Domb and J. Lebowitz (eds) Phase Transitions and Critical Phenomena, Vol. **13** (Academic Press, New York).
- [10] M.F. Sykes, D.S. Gaunt, P.D. Roberts and J.A. Wyles, J. Phys. **A5** (1972) 624.
- [11] M. E. Fisher and H. Au-Yang, J. Phys. **A** (1979) 1677; D. L. Hunter and G. A. Baker, Phys. Rev. **B 19** (1979) 3808.
- [12] C.F. Baillie, R. Gupta, K.A. Hawick and G.S. Pawley, Phys. Rev. **B45** (1992) 10438.
- [13] A.J. Liu and M.E. Fisher, J. Stat. Phys. **58** (1990) 431.